ChemMedChem

Chemistry Europe
European Chemical Societies Publishing

Accepted Article

Title: Red Emissive Carbon Dots Prepared from Polymers as An Efficient Nanocarrier for Coptisine Delivery In Vivo and In Vitro

Authors: Wei Ren, Fuchun Nan, Shumu Li, Sijin Yang, Jiechao Ge, and Zhenwen Zhao

To be cited as: *ChemMedChem* 10.1002/cmdc.202000420

Link to VoR: https://doi.org/10.1002/cmdc.202000420

WILEY-VCH

FULL PAPER WILEY-VCH

Red Emissive Carbon Dots Prepared from Polymers as An Efficient Nanocarrier for Coptisine Delivery *In Vivo* and *In Vitro*

Wei Ren[a, b, c], Fuchun Nan[d], Shumu Li[b, c], Sijin Yang[a*], Jiechao Ge[d*] and Zhenwen Zhao[b, c*]

[a] W. Ren, Prof. S. Yang
National Traditional Chinese Medicine Clinical Research Base, Affiliated Traditional Chinese Medicine Hospital
Southwest Medical University
Luzhou 646000 (China)
E-mail: ysjimn@sina.com

[b] W. Ren, Dr. S. Li, Prof. Z. Zhao
Beijing National Laboratory for Molecular Sciences, CAS Research/Education Center for Excellence in Molecular Sciences
Key Laboratory of Analytical Chemistry for Living Biosystems
Institute of Chemistry Chinese Academy of Sciences, Beijing Mass Spectrum Center
Beijing 100190 (China)
E-mail: zhenwenzhao@iccas.ac.cn

[c] W. Ren, Dr. S. Li, Prof. Z. Zhao
Graduate School
University of Chinese Academy of Sciences
Beijing 100190 (China)
E-mail: zhenwenzhao@iccas.ac.cn

[d] F. Nan, Prof. J. Ge
Key Laboratory of Photochemical Conversion and Optoelectronic Materials and CityU-CAS Joint Laboratory of Functional Materials and Devices Technical Institute of Physics and Chemistry
Chinese Academy of Sciences
Beijing 100190 (China)
E-mail: jchge2010@mail.ipc.ac.cn

Abstract: Negatively charged fluorescent carbon dots (CDs, E_m=608 nm) were hydrothermally prepared from thiophene phenylpropionic acid polymers and then successfully loaded with the positively charged anticancer cargo coptisine, which suffers from poor bioavailability. The formed CDs-Coptisine complexes were thoroughly characterized by particle size, morphology, drug loading efficiency, drug release, cellular uptake and cellular toxicity *in vitro* and anti-tumor activities *in vivo*. In this nano-carrier system, red emissive CDs possesses multiple advantages as follows: 1) high drug loading efficiency (>96%); 2) sustained drug release; 3) enhanced drug efficacy towards cancer cells; 4) EPR effect; 5) drug release tracing with near-infrared imaging. These properties indicated that red emissive CDs prepared from polymers could be used as a novel drug delivery system with integrated therapeutic and imaging functions in cancer therapy, which are expected to have great potential in future clinical applications.

Introduction

Cancer is a world major disease, posing a great threat to human health.[1] Currently, nanomaterials based drug delivery systems have been widely developed to improve the therapeutic efficacy against cancers.[2] Among them, nanocarriers with intrinsic fluorescent properties were excellent candidates for real-time tracking, simultaneous diagnosis and therapy.[3] As a newly emerging star gaining increasing attention, fluorescent carbon dots (CDs) were firstly discovered during the separation and purification of single-walled carbon nanotubes in 2004 and further received their name ''carbon dots'' in 2006.[4] Owing to their unique merits including non-blinking photoluminescence (PL) emission, high photostability, low cytotoxicity, excellent biocompatibility, eminent water solubility and easy functionalization,[5] CDs showed great advantages compared to the traditional organic dyes and inorganic quantum dots. As a result, CDs have revealed a great deal of applications in biomedical areas including cancer therapy,[6] bio-imaging[7] and drug delivery.[8] For biomedical applications, red or near-infrared emissive CDs with long wavelength could be highly beneficial because emissions in the red emissive window would yield significant improvement in the tissue-penetration depth for *in vivo* bioimaging.[9] However, synthesis of red emissive CDs still stands as a major challenge.[10]

As CDs contain a large proportion of functional groups such as -NH_2, -OH and -COOH[11] on their surface, consequently, it is possible for CDs to carry many therapeutics.[12] Though many researches have applied CDs for drug delivery, it is mainly focused on the use of green or blue CDs for the delivery of doxorubicin.[13] Moreover, CDs prepared from well defined polymers can endow them with controlled surface morphology, polymeric structures and unique properties.[14] However, to the best of our knowledge, few research on the application of polymers based red emissive CDs as nano-carriers of other anticancer drug cargos has been reported so far.

Coptisine is a positively charged alkaloid extracted from *Coptis chinensis*, sharing the same molecular skeleton with berberine. Several evidences suggest that coptisine possesses anti-tumor activities towards various kinds of cancers including human pancreatic cancer,[15] lung cancer,[16] colorectal cancer[17] and hepatocellular carcinoma.[18] However, the oral delivery of most protoberberine alkaloids including coptisine is hindered by their low gastrointestinal absorption, limiting their clinical applications and translation.[19] In our previous work, red emissive CDs were prepared as a novel phototheranostic agent for effective tumor imaging and therapy.[3a] Simultaneously, we discovered that N and S elements doping is an effective approach to obtain red emissive CDs and the electrostatic attraction coupled with π-π interactions between the oppositely charged CDs and surfactant molecules could form CDs-surfactant complexes.[20] Further, we successfully constructed a multifunctional nano-carrier system using red emissive CDs encapsulated liposomes with integrated therapeutic and imaging

functions.[21] However, more extensive and deep-going explorations of the applications of red emissive CDs are still needed. Inspired by our previous findings, we hypothesized that the positively charged coptisine could be loaded onto the negatively charged CDs, making it possible to construct a multifunctional nano-system integrating the fluorescent properties of CDs and the anticancer function of coptisine into a single unit.

In this study, red emissive CDs were synthesized by hydrothermal method using thiophene phenylpropionic acid polymers as the carbon source. Then, the CDs were loaded with coptisine to prepare CDs-Coptisine complexes as a novel drug delivery nano-system for cancer treatment. The prepared CDs-Coptisine complexes were thoroughly characterized by various spectroscopic and microscopic techniques. In addition, the *in vitro* anticancer effect, the cellular uptake of the CDs-Coptisine complexes were investigated. Finally, *in vivo* bio-imaging and anti-tumor activity of the CDs-Coptisine complexes were performed by tumor bearing nude mice. Cumulatively, for the first time we demonstrated the utility of polymers based red emissive CDs as a novel drug delivery system for the simultaneous drug delivery, cellular imaging and drug tracking of the protoberberine alkaloid coptisine (Scheme 1), which may broaden the applications of CDs in biomedical fields.

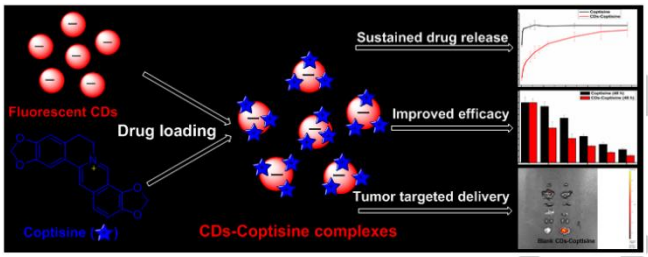

Scheme 1. Schematic illustration of polymers based red emissive CDs loading coptisine for efficient cancer therapy.

Results and Discussion

Characterization of red emissive CDs and coptisine

The hydrothermal synthesis of red emissive CDs from polymers just followed our previously developed procedures as shown in Figure S1.[20, 22] The prepared CDs appear spherical and are highly water soluble and good dispersion, with a size ranging from 5 to 8 nm (Figure 1A). The UV-vis absorption spectrum of CDs showed that a broad absorption peak exists at 440 nm (Figure 1B), which was assigned to the n–π* transition from the surface groups and was consistent with our previous reports.[21-22] The photoluminescence (PL) emission spectrum of the CDs had a wide range from 550 to 700 nm with a peak at 608 nm, exhibiting the excitation-independent PL behavior, which was related to the surface states/groups of the CDs (Figure 1B).[20] In addition, the CDs showed the largest PL intensity when excited at 380 nm (Figure 1C), as the excitation wavelength further increases, the PL intensity gradually decreases. Furthermore, the stability of CDs was investigated and the results showed that the prepared CDs were stable in a phosphate buffered saline (PBS) solution as shown in Figure 1D.

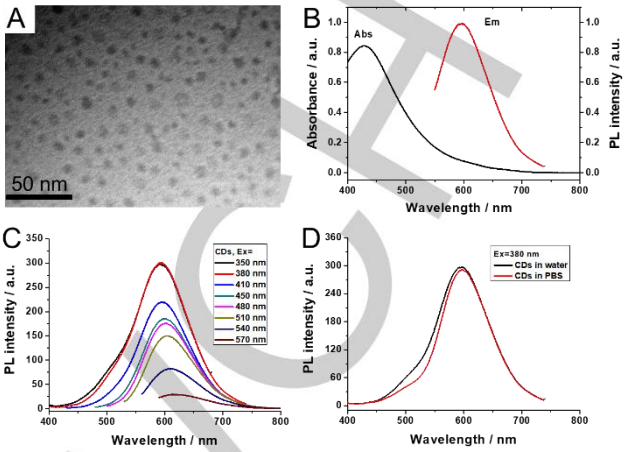

Figure 1. (A) HR-TEM image of CDs; (B) UV-vis absorption (black) and PL emission (red) spectra of CDs; (C) PL emission spectra of CDs at different excitation wavelengths from 350 to 570 nm; (D) PL stability of CDs in water and PBS solution.

For coptisine, it had two emission peaks with the main peak at 446 nm and a minor peak at 550 nm under different excitation wavelengths (Figure S2A). When the emission peak is 446 nm, the maximum absorption wavelength of coptisine is 338 nm and 380 nm (Figure S2B). Consequently, 380 nm was chosen as the optimal excitation wavelength in further experiments. The stability investigation showed that coptisine was also stable in a PBS solution (Figure S2C).

Investigation of the drug loading property of the prepared CDs

As a quaternary ammonium alkaloid, coptisine was a positively charged compound. For CDs, they were negatively charged nanoparticles as the carbon source of the CDs phenylpropionic acid (PPA) polymers contained plenty of -COOH.[22] Consequently, it was inferred that the positively charged coptisine could be loaded onto the negatively charged CDs via electrostatic attractions and other interactions.

Based on our hypothesis, the drug loading property of the prepared CDs was investigated firstly. To be specific, different concentrations of CDs (2.5-100 μg/mL) were used to mix with coptisine and the drug loading capacity of various concentrations of CDs were investigated. As shown in Figure 2A, when the concentration of coptisine was fixed at 10 μg/mL, the drug binding percentage of coptisine gradually increased as the concentration of CDs ranged from 2.5 μg/mL to 100 μg/mL. When the concentration of CDs was 100 μg/mL, the drug binding percentage of coptisine was as high as 96.8%, demonstrating excellent drug loading property of the prepared CDs. Further, the morphology of CDs-Coptisine complexes was investigated by TEM. The images revealed that the CDs-Coptisine complexes were homogeneously distributed and possessed sizes of around 5-8 nm with well-defined spherical shape as that of CDs (Figure 2B). Meanwhile, the zeta potential

of CDs, coptisine and CDs-Coptisine complexes was investigated as shown in Figure 2C. As a quaternary ammonium alkaloid, the zeta potential of coptisine was + 4.7 mV, after being loaded onto the negatively charged CDs (- 37.9 mV), the zeta potential of the CDs-Coptisine complexes was - 12.8 mV, which was an evidence of the successful loading of coptisine onto CDs. Furthermore, the FT-IR analysis of CDs, coptisine and CDs-Coptisine complexes shown in Figure 2D also explicitly demonstrated the successful loading of coptisine onto CDs.

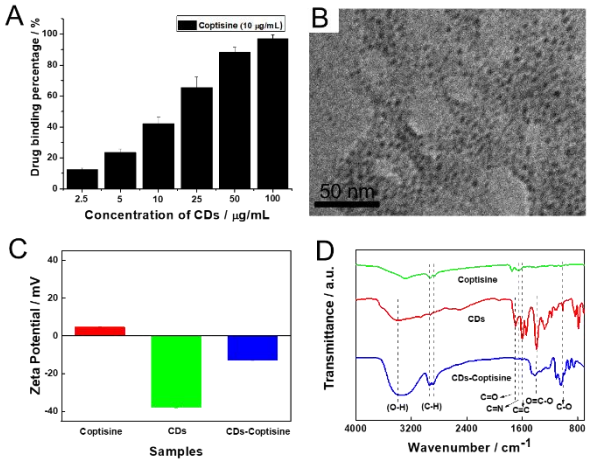

Figure 2. (A) Drug binding percentage of coptisine with different concentrations of CDs; (B)TEM images of CDs-Coptisine complexes; (C) Zeta potential of coptisine, CDs and CDs-Coptisine complexes; (D) FT-IR spectra of coptisine, CDs and CDs-Coptisine complexes.

To further verify the university of drug loading property of the negatively charged CDs, two other positively charged compounds including berberine and palmatine (Figure S3) were mixed with CDs and their drug binding percentages were calculated. The results showed that the drug binding percentages of berberine and palmatine onto CDs were both above 96% (Figure S4) at a proper CDs/coptisine ratio, further demonstrating excellent drug loading property of the prepared CDs. Thus, due to the high drug loading capacity, the polymers based CDs provided an ideal delivery system for cancer therapy.

Optical characterization of CDs-Coptisine complexes

In the study, the optical properties of CDs-Coptisine complexes were investigated after coptisine was loaded onto CDs. Figure 3A showed the photos of CDs, coptisine and CDs-Coptisine complexes under daylight and UV light irradiation (254 nm). Under normal light, the CDs and CDs-Coptisine solution was rufous and the coptisine solution was clear. Under UV illumination, after forming CDs-Coptisine complexes, an obvious color change was observed, indicating the PL change of CDs and coptisine. It can be observed from Figure 3B that there were two absorption peaks centered around 350 nm and 450 nm in the UV-vis spectrum of CDs-Coptisine complexes, which was due to the absorption combination of coptisine at 350 nm and CDs at 450 nm, indicating that coptisine was successfully loaded onto CDs. As shown in Figure 3C, the PL emission of coptisine decreased after mixed with CDs at excitation of 380 nm. It should be noted that there is energy transfer between CDs and coptisine in theory. The absorbance peak of CDs appears at 450 nm, and the fluorescence peak of coptisine appears at 446 nm. The match of the donor and acceptor maxima appears to support an obvious fluorescence resonance energy transfer process from coptisine to CDs. As shown in Figure 3C, the PL intensity of coptisine at 446 nm decreased after mixed with CDs. As the concentration of CDs increased, the PL intensity of coptisine further decreased. After mixed with coptisine, the PL intensity of CDs also decreased (Figure 3D) to some extent, which may construct an “off-on” system to track the drug release of coptisine from CDs-Coptisine complexes. The PL emission spectrum of CDs-Coptisine complexes shared the same peak at 608 nm with CDs when excited at different wavelengths (Figure S5). Furthermore, the UV-vis absorption and PL spectra of CDs-Coptisine complexes in a PBS solution were almost the same as those in water suspension (Figure 3B and Figure S6), indicating that the CDs-Coptisine complexes were stable in a PBS solution.

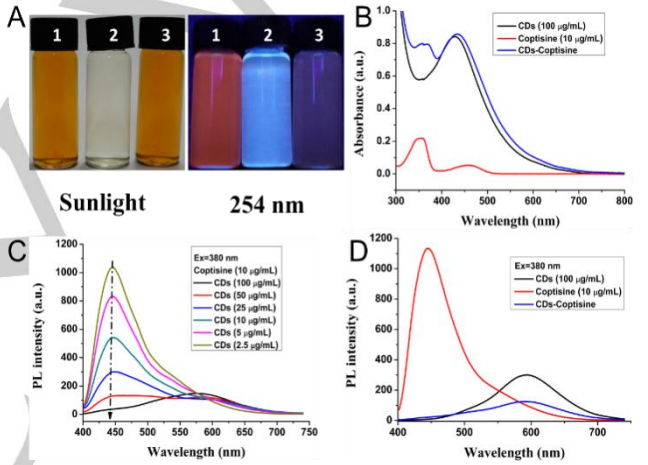

Figure 3. (A) Photographs of (1) CDs (100 μg/mL), (2) coptisine (10 μg/mL) and CDs-Coptisine complexes (3) under daylight and UV illumination; (B) UV-vis absorption spectra of CDs, coptisine and CDs-Coptisine complexes; (C) PL spectra of coptisine (10 μg/mL) after mixed with different concentrations of CDs (2.5-100 μg/mL) at excitation of 380 nm; (D) PL spectra of coptisine (10 μg/mL), CDs (100 μg/mL) and CDs-Coptisine complexes at excitation of 380 nm.

In vitro drug release and cytotoxicity of CDs-Coptisine complexes

Prior to experiments, an ultra-high performance liquid chromatography-Qtrap mass spectroscopy (UPLC-Qtrap-MS) method was established for the determination of coptisine as well as its analogues berberine and palmatine (Figure 4A and Figure S7) in this study. The MS/MS parameters were shown in Table 1. The calibration curve of coptisine showed an excellent correlation between the peak area and concentration within the test ranges (Figure 4B). The *in vitro* drug release behavior of coptisine after being loaded onto CDs was investigated in PBS buffer (pH=7.4) at 37 °C. Coptisine dissolved in methanol was used as a control, which was the same concentration as presented in CDs-Coptisine complexes. As depicted in Figure 4C, coptisine was slowly released after being loaded onto CDs. The free coptisine exhibited 90% release after 4 h, while the

CDs-Coptisine complexes exhibited very slow release of 38% in the first 4 h, followed by the slow release of coptisine after 48 h under neutral condition, demonstrating sustained drug release property of the CDs-Coptisine complexes.

Table 1. MS/MS parameters for quantification of coptisine, berberine and palmatine using UPLC-Qtrap-MS.

Compounds	RT[a]	Q1[b]	Q3[c]	DP[d]	CE[e]	ST[f]
Coptisine	7.8	320	277	150	46	200
Berberine	8.9	336	292	130	42	200
Palmatine	8.7	352	308	220	40	200

[a] Retention time (RT, min). [b] Precursor ion (Q1, *m/z*). [c] Product ion (Q3, *m/z*). [d] Declustering potential (DP, V). [e] Collision energy (CE, eV). [f] Scan time (ST, ms).

The *in vitro* cytotoxicity of free coptisine and CDs-Coptisine complexes were measured by MTT assay using MCF-7 cells. As a kind of heavy metal-free nanotheranostics material, CDs were considered to be advantageous over heavy metal quantum dots with respect to biocompatibility and low toxicity. As reported in our previous reports,[20-22] 200 μg/mL of CDs did not cause any significant cytotoxicity to normal bronchial epithelial cells (HBE) and human cancer cells (HeLa, MCF-7 and HepG2 cells). As shown in Figure 4D, pure coptisine demonstrated a dose-dependent cytotoxic effect within the ranges from 2 μg/mL to 20 μg/mL against MCF-7 cells. In comparison, the CDs significantly enhanced the dose-dependent cytotoxic effect of coptisine within the test ranges. To verify the universality of the cytotoxic effect of CDs-Coptisine drugs to cancer cells, two other cancer cell lines, namely, HepG2 cells and HCT116 cells were also employed for the same set of evaluations. As shown in Figure S8, both coptisine and CDs-Coptisine complexes showed a dose-dependent cytotoxic effect towards HepG2 cells and HCT116 cells. After being loaded onto CDs, coptisine showed enhanced antitumor efficacy compared with coptisine alone at different concentrations from 1 μg/mL to 20 μg/mL.

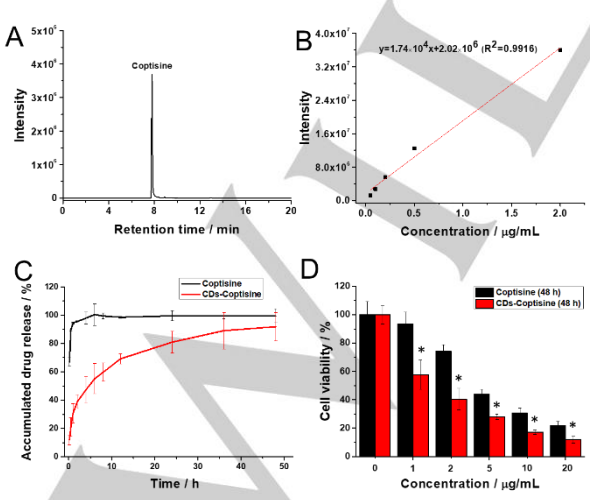

Figure 4. (A) Typical extracted ion chromatogram of coptisine using UPLC-Qtrap-MS; (B) Standard curve of coptisine established by UPLC-Qtrap-MS; (C) In vitro cumulative coptisine release from CDs-Coptisine complexes in PBS; (D) Cellular cytotoxicity assessment of coptisine and CDs-Coptisine complexes against MCF-7 cells. Student's t-test was performed between saline group and CDs-Coptisine conjugates group (*p<0.01).

In vitro cellular examination of CDs-Coptisine complexes

In order to determine the localization of CDs-Coptisine complexes in cells, a fluorescence imaging study of MCF-7 and HepG2 cells incubated with CDs-Coptisine complexes was performed. Figure 5A and 5B showed confocal images of MCF-7 and HepG2 cells treated with CDs-Coptisine complexes at bright field and excitation wavelengths of 559 nm, respectively. The images clearly showed that the CDs loaded with coptisine were observable in the cells after co-incubation in both MCF-7 and HepG2 cells, mainly in the cytoplasm, which was consistent with our previous studies.[21-22]

Further, the content of coptisine in a single cell after cellular uptake of CDs-Coptisine complexes at different time points was determined using UPLC-Qtrap MS in MCF-7 cells and HepG2 cells (Figure 5C and 5D), which was the first attempt to calculate the content of coptisine in a single cell. After 2 h incubation, the content of coptisine was 0.19 pg/cell in MCF-7 cells and 0.20 pg/cell in HepG2 cells, respectively. After 5 h incubation, the content of coptisine was 0.26 pg/cell in MCF-7 cells and 0.25 pg/cell in HepG2 cells, respectively. The results verified the existence of coptisine in MCF-7 cells and HepG2 cells by UPLC-Qtrap MS.

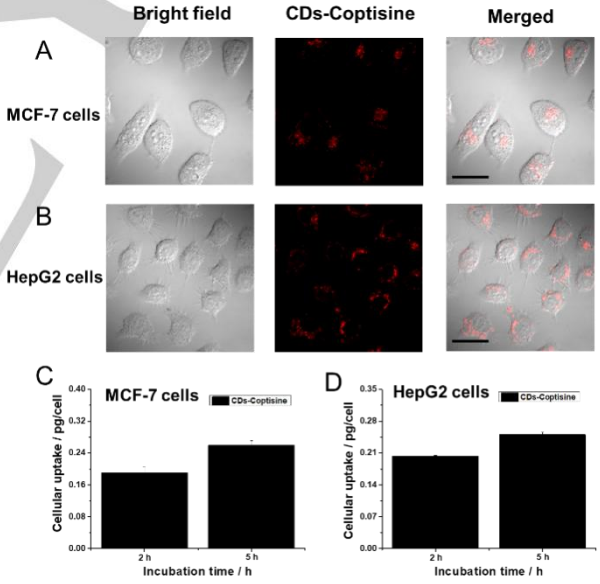

Figure 5. CLSM images of (A) MCF-7 cells and (B) HepG2 cells incubated with CDs-Coptisine complexes (concentration of coptisine: 10 μg/mL) for 5 h. The scale bar corresponds to 30 μm; (C) Concentration of coptisine after cellular uptake of CDs-Coptisine complexes at different time points in MCF-7 cells and (D) HepG2 cells.

In vivo antitumoral activity and biodistribution of the CDs-Coptisine complexes

The therapeutic outcomes were evaluated by monitoring the tumor volumes and body weights of the mice every other two days for 18 days. Coptisine and CDs-Coptisine complexes

showed antitumor activity in the MCF-7 tumor model. As illustrated in Figure 6A, the tumor growth was significantly inhibited by coptisine and CDs-Coptisine complexes after the first four caudal vein administrations as revealed by the reduced tumor volume in comparison with that of the saline group. However, no significant tumor volume difference was observed at days 15 and 18 after the last two caudal vein administrations of coptisine by comparison with the saline group. And CDs could enhance the anticancer anticancer activity of coptisine. In addition, the loss of body weight was analyzed as an indicator for treatments-induced toxicity. As shown in Figure 6B, no obvious body weight change was observed in the mice for the groups, which indicated that the nano-system had no obvious systemic toxicity.

Moreover, we also studied the biodistribution of CDs-Coptisine complexes by monitoring the PL of CDs in the tumor and other major organs excised from the mice. As shown in Figure 6C, the excised tumor tissue showed strong PL intensity, whereas the heart, spleen, lung and kidney showed very low signals. These results demonstrated that the CDs-Coptisine complexes could specifically target the tumor site through the EPR effect [23] after intravenous injection, which were very advantageous to realize imaging-guided drug delivery with high therapeutic efficiency and low toxic side effects.

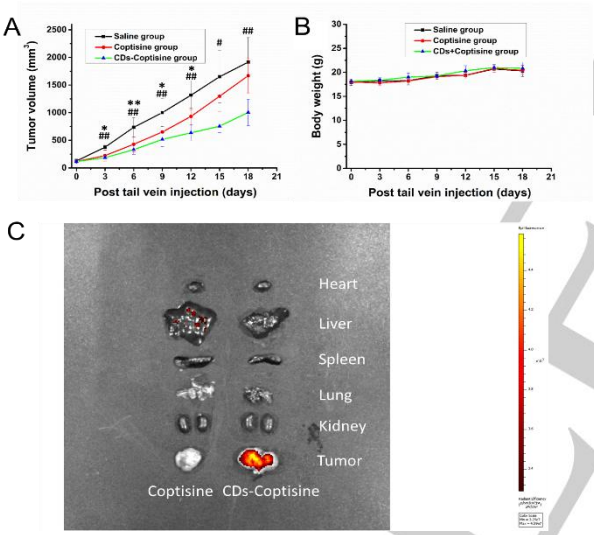

Figure 6. (A) Tumor growth curves of rats in the saline group, coptisine group and CDs-Coptisine complexes group; (B) Body weight of rats in the saline group, coptisine group and CDs-Coptisine complexes group; (C) *Ex vivo* images of mice tissues (from top to bottom: heart, liver, spleen, lung, kidney and tumor) 24 h post tail intravenous injection of coptisine (the left) and CDs-Coptisine complexes (the right). The color bars represent the PL intensity. Student's t-test was performed between saline group and coptisine group (*****p<0.05, ******p<0.01), as well as between coptisine group and CDs-Coptisine complexes group ($^{\#}p$<0.05, $^{\#\#}p$<0.01).

In addition, we have examined the *in vivo* imaging ability of CDs-Coptisine complexes via intratumor injection in MCF-7 bearing nude mice. As can be seen in Figure 7, an obvious PL signal was detected at the injection site in 6 h after intratumor injection, and enhanced PL was observed at 24 h, which was owing to the drug release of coptisine from CDs-Coptisine complexes and then PL recovery of CDs. Consequently, the PL of CDs could be used to track drug release of CDs-Coptisine complexes *in vivo*.

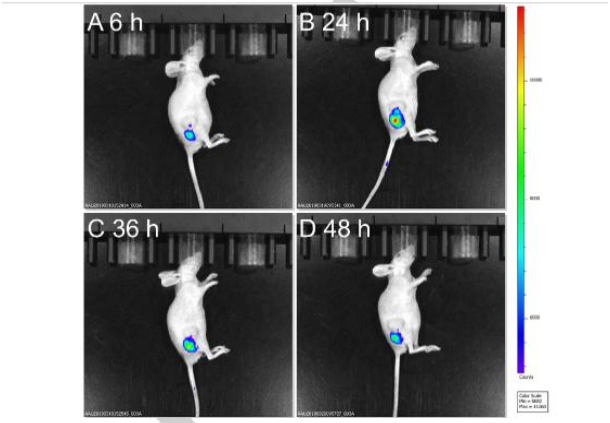

Figure 7. (A-D) *In vivo* PL images of nude mice treated with intratumor injection of 100 μL of CDs-Coptisine complexes at different points (6 h, 24 h, 36 h and 48 h) post injection, respectively.

Over the past decade, many reports have demonstrated that protoberberine alkaloids like coptisine and berberine had high activity against various kinds of cancer.[24] For example, coptisine was reported to inhibit colorectal cancer growth and progression by down-regulating MFG-E8[17a] and exert an anti-cancer effect on hepatocellular carcinoma by up-regulating miR-122.[18a] Huang tao *et, al.* suggested that coptisine may be potential as a novel anti-tumor candidate in the HCT-116 cells-related colon cancer.[25] However, the conventional approach like chemotherapy generally lacks specificity and causes toxicity and multidrug resistance problems. Therefore, there is a strong need for the development of effective drug delivery system to overcome the limitations.

In recent years, nanotechnology has provided the convenient tools for nanoparticle-mediated combination therapy to induce synergistic drug actions and deter the onset of drug resistance.[26] CDs are fascinating nanoparticles with intrinsic fluorescent properties that can serve a dual function of bioimaging and drug delivery with minimal concerns about cytotoxicity.[13a, 27] CDs have extremely high surface area to volume ratios, making them ideal candidates for drug loading and delivery.[28] Thus, CDs became a preferable choice in various biomedical applications,[29] especially for the polymers based CDs with controlled surface chemistry and polymeric structures.[14a, 14b] However, to the best of our knowledge, the application of red emissive CDs prepared from polymers for the drug delivery of drug cargos like coptisine has been rarely reported so far. In the present study, red emissive CDs prepared from polymers possessing unique properties were used as the nanocarrier of coptisine for the first time. From the results and analysis of both the *in vitro* cellular cytotoxicity and *in vivo* tumor inhibition experiments, it can be inferred that our CDs provide a smart drug carrier system in cancer therapy, affording both trackability and targeted drug delivery. This study provided evidence supporting that red emissive CDs prepared from polymers held great potential in targeted drug delivery for cancer therapy with low systemic toxicity. Therefore, our study would broaden the application of CDs in biomedical fields.

Conclusion

In summary, we successfully developed a red emissive polymer CDs based nano-carrier system with integrated functions for simultaneous imaging and drug delivery *in vivo* and *in vitro*. In this nano-carrier system, red emissive CDs possesses multiple functions including drug carrier, EPR effect and simultaneous imaging. The *in vitro* experiments revealed that polymers based red emissive CDs could achieve a sustained drug release effect and enhance drug efficacy of coptisine toward cancer cells. Further *in vivo* study demonstrated the suitability of the fluorescent CDs as a tumor targeted drug delivery carrier and drug release tracer of coptisine for cancer therapy. It is believed that the present CDs-based nano-system will hold great potential in the development of highly biocompatible and tumor targeted drug delivery system for cancer therapy in the clinic with minimal side effects and toxicity.

Experimental Section

Chemicals and reagents

Berberine, coptisine and palmatine were purchased from Beijing Saibaicao Co., Ltd. (Beijing, China). Purities of all compounds were above 98% by HPLC analysis. 1-(4,5-dimethylthiazol-2-yl)-3,5-diphenylformazan (MTT) was purchased from Sigma-Aldrich (St. Louis, MO, USA). HPLC grade methanol, acetonitrile and MS grade formic acid were purchased from Thermo Fisher Scientific (Pittsburgh, PA, USA). Ultrapure water was obtained from a Milli-Q water purification system (Millipore Corporation, USA). All other chemicals and reagents were from commercial sources unless otherwise described. MCF-7 cells, HepG2 cells and HCT 116 cells were obtained from the national experimental cell resource sharing platform (Beijing, China). Dulbecco's modified eagle medium, fetal bovine serum and trypsin were purchased from Invitrogen Gibco (Carlsbad, CA, USA). Female BALB/c nude mice were provided by Cisco North Biotechnology Co., Ltd. (Beijing, China).

Instrumentation

The fluorescent intensity was detected on the F-4500 fluorescence spectroscopy (Hitachi, Japan). Ultraviolet-visible absorption spectra were measured using a TU-1900 UV-vis double-beam spectrometer (Purkinje General, China). Zeta potential was recorded with Zetasizer Nano-ZS ZEN3600 spectrometer (Malvern, UK). High-resolution transmission electron microscopy (HRTEM) photos were recorded with JEM-2100F operating at 200 kV. Attenuated total reflection FTIR spectra were recorded on a Thermo Scientific Nicolet 6700 FT-IR spectrometer, over the range of 400-4000 cm^{-1}. Confocal laser scan microscopy (CLSM) observations were performed using a confocal laser scanning biological microscope FV1000-IX81 (Olympus, Japan). A digital camera was used to capture the photographs of solutions.

Preparation of red emissive CDs and CDs-Coptisine complexes

The hydrothermal synthesis of red emissive CDs just followed our previously developed procedures[20, 22] as shown in Figure S1. In brief, thiophene phenylpropionic acid (PPA) monomers were prepared initially via a suzuki reaction using thiophene-3-boronic acid and 3-(4-Bromophenyl) propionic acid under the catalysis of $Pd(PPh_3)_4$. Subsequently, PPA polymers were prepared via an oxidative polymerization of PPA monomers under the catalysis of $FeCl_3$. Finally, CDs were prepared by hydrothermal treatment of PPA polymers, which was dissolved in alkaline solution, and then heated to 240 °C for 36 hours. After cooling to room temperature, the resultant CDs solution was filtered through a Millipore 0.22 μm filter and then dispersed in water for further characterization and evaluation. For the determination of the CDs' concentration, certain volume of the solution containing CDs was taken (V) and dried under vacuum. Then the weight of the dried CDs was accurately weighed (m). Finally, the concentration of the CDs solution (C) was calculated following the formula: C=m/V.

Further, coptisine was loaded onto prepared CDs by electrostatic interactions or hydrogen bonding.[13b, 13c] Firstly, 1 mL of coptisine (20 $\mu g \cdot mL^{-1}$) was mixed with 1 mL of various concentrations of CDs individually (from 5 $\mu g \cdot mL^{-1}$ to 200 $\mu g \cdot mL^{-1}$) in phosphate buffer saline (PBS, pH=7.4) under stirring to form a final solution system of 2 mL. This solution was then allowed to react for 24 h on an incubator shaker (Crystal, China), set to 200 rpm at 24 °C in the dark. Then the free coptisine was removed via ultrafiltration (Amicon Ultra-4, MW=3 kDa; Millipore, MA, USA) at 4000 g for 20 minutes. The prepared CDs-Coptisine solution was maintained at 4 °C in the dark, until needed for further experiments. To verify the drug loading ability of CDs, another two positively charged alkaloids including berberine and plamatine were loaded onto CDs as well. The procedure was the same as that of coptisine.

Determination of coptisine loading efficiency (LE)

The LE of coptisine was determined using the ultrafiltration method.[30] In brief, 0.2 mL of unultrafiltrated CDs-Coptisine solution was added into the centrifugal filter device (Amicon Ultra-0.5, MW=3 kDa; Millipore, MA, USA) and centrifuged at 12000 g for 20 minutes. The ultrafiltrate was collected and subjected to UPLC-Qtrap-MS quantification to obtain free drug concentration [C_{free}]. The CDs loaded with coptisine was collected and extracted with 0.2 mL of methanol by ultrasonication for 15 minutes. Followed by centrifugation at 12000 g for 15 minutes, the ultrafiltrate was collected and subjected to UPLC-Qtrap-MS quantification to obtain loaded drug concentration [C_{loaded}]. The procedure for the LE determination of berberine and palmatine was the same as that of coptisine. The LE of coptisine, berberine and palmatine was calculated according to the following formula:

$$LE\ (\%) = \frac{[C_{loaded}]}{[C_{free}]+[C_{loaded}]} \times 100$$

The concentrations of coptisine, berberine and palmatine in solutions and biological samples were quantified using MRM mode from an AB Sciex Qtrap® 4500 tandem MS (Foster, CA, USA) equipped with an ESI source connected to the UPLC system (I-class Acquity ultra performance liquid chromatography, Waters). The chromatographic condition was shown in Table S1. Qtrap MS was operated in the positive ion mode. The MRM ion pairs and corresponding DP and CE of coptisine, berberine and palmatine were optimized and presented in Table 1. The peak areas of different concentrations of coptisine (50 ng/mL-2 μg/mL) analyzed by UPLC-Qtrap-MS were collected to establish standard curve and further calculate the concentrations of each analyte in real samples.

In vitro drug release

Drug release study was performed using a dialysis technique as described earlier.[21, 30] In brief, 1 mL of ultrafiltrated CDs-Coptisine complexes (concentration of CDs: 2 mg/mL; concentration of coptisine: 193.6 μg/mL) was put into a dialysis bag (molecular weight cut-off of 3.5 kDa). PBS solution (pH=7.4, 500 mL) maintained at 37 °C was used as the release medium under magnetic stirring. At timed intervals, the concentration of coptisine was quantified by UPLC-Qtrap MS as described above. The release curve was plotted with cumulative drug release as the function of time. Similar experiment was carried out by use of free coptisine (the same concentration as that of coptisine in CDs-Coptisine complexes, namely, 193.6 μg/mL) that dissolved in methanol.

Intracellular uptake of coptisine

The intracellular uptake of coptisine was investigated by quantification of coptisine in the cells. Namely, HepG2 cells and MCF-7 cells were seeded into cell culture flasks at a density of 3.0×10^6 cells/flask. After 24 h pre-incubation, cells were treated with CDs-Coptisine complexes for 2 h or 5 h at the concentration of 10 μg/mL (coptisine equivalent). Then, cells were washed with PBS for five times and harvested by trypsinization. After sonication in 200 μL of methanol for 5 min, cells were centrifuged at 12000 g for 10 min to collect supernatant containing coptisine, which was quantified by UPLC-Qtrap-MS as described above. In addition, the intracellular uptake of CDs-Coptisine complexes was also analyzed by the fluorescence of CDs using a fluorescence Microscope (Olympus, Japan). Namely, HepG2 cells and MCF-7 cells were placed onto glass-bottom cell culture dishes (r=15 mm) at a density of 5×10^4 cells per dish and were allowed to adhere at 37 °C for 24 h before treatment. Then, HepG2 cells and MCF-7 cells were incubated with CDs-Coptisine complexes (the concentration of coptisine: 10 μg/mL) in fresh culture without serum and antibiotics at 37 ^{o}C. After 5 h incubation, PBS was used to wash the cells three times and observed for CLSM imaging. The method of point illumination was achieved by laser beam and objective lens. The excitation source was set as FV10-LD559 (559 nm) and the laser power was set to be 20 mw. The emission filter was BA575 (Olympus) and the wavelength range of 575-675 was collected. The detector was photoelectric multiplier (PMT), which was synchronized with scanning mirrors.

***In vitro* cytotoxicity assay**

The MTT-based assay was performed to compare the cytotoxicity of coptisine and CDs-Coptisine complexes *in vitro*. For cytotoxicity assay, MCF-7 cells and HepG2 cells in logarithmic growth were plated in 96-well plates at a density of 6×10^3 cells per well in 100 μL of culture medium and were allowed to adhere for 24 h before treatment. Serial concentrations of each sample (coptisine and CDs-Coptisine complexes) were then added (100 μL per well). After treated for 48 h, MTT solution (10 μL per well, 5 mg/mL) was added to each well and incubated for 4 h at 37 °C. The supernatant was then carefully removed, and 150 μL of dimethyl sulfoxide was added to each well. After the formazan crystals had dissolved completely, optical density at 570 nm was determined with a SpectraMax 190 microplate reader (Molecular Devices, Sunnyvale, CA, U.S.A). The cell viability was calculated as a percentage from the viability of the control (untreated) cells. The viability of the control cells was considered as 100%.

***In vivo* imaging and biodistribution of CDs-Coptisine complexes**

Hereby, we declared that all the animal experiments were performed in compliance with the relevant laws and institutional guidelines and the protocol was approved by the Ethics Committee of Institute of Chemistry Chinese Academy of Sciences. Firstly, a subcutaneous MCF-7 tumor was established by injecting a suspension of 2×10^7 MCF-7 cells in PBS (100 μL) into the buttock of each female BALB/c nude mouse (4-week-old, 16 g-18 g) and was allowed to grow for 10 days. When the tumors reached approximately 200 mm^3, the mice were treated with intratumor or tail intravenous injections of 100 μL of CDs-Coptisine complexes. The nude mice injected with 100 μL of saline were selected as controls. The mice PL imaging experiments were successfully performed at different time points (6, 24, 36 and 48 h) post intratumor injection using a PerkinElmer *in vivo* imaging system with 500 nm excitation light and a 600 nm emission. Prior to imaging, we firstly obtained pre-contrast data with excitation under the same excitation and emission wavelength ranges. Besides, to investigate the biodistribution of CDs-Coptisine complexes, the mice intravenously injected with coptisine and CDs-Coptisine complexes were sacrificed by exsanguinations at 24 h post-injection, and the tumor and major organs (hearts, livers, spleens, lungs, and kidneys) were harvested for *ex vivo* PL imaging.

***In vivo* study of the therapeutic efficacy**

MCF-7 tumor-bearing mice were prepared for evaluating the *in vivo* antitumoral activity of CDs-Coptisine. When the tumor volume reached 200 mm^3, 18 mice were divided into three groups: saline group (5.0 mL/kg, n=6), coptisine group (10 mg/kg, n=6) and CDs-Coptisine complexes group (10 mg coptisine/kg, n=6), on the basis of the solutions they were administered by intravenous injection through the vena caudalis every 3 days for 18 days. In the course of treatment, the body weights and tumor sizes were recorded once every two days and the tumor volumes (V) were calculated according to the formula:

$$V = 0.52 \times \text{length} \times \text{width}^2$$

Statistical analysis

The statistical significance of the data was compared by Student's t-test. All values were expressed as mean ± SD. $p<0.05$ was considered statistically significant.

Acknowledgements

This work was supported by the National Natural Science Foundation of China (Grant No. 21575146, 51972315 and 81703905) and the Strategic Priority Research Program of the Chinese Academy of Sciences (Grant No. XDB17000000).

Conflict of Interest

There are no conflicts to declare.

Keywords: carbon dots • coptisine • nanoparticles • drug delivery • near infrared imaging

[1] F. Bray, J. Ferlay, I. Soerjomataram, R. L. Siegel, L. A. Torre, A. Jemal, *CA Cancer J Clin* **2018**, *68*, 394.

[2] a) E. B. Manaia, M. P. Abucafy, B. G. Chiari-Andreo, B. L. Silva, J. A. Oshiro Junior, L. A. Chiavacci, *Int J Nanomedicine* **2017**, *12*, 4991; b) D. B. Vieira, L. F. Gamarra, *Int J Nanomedicine* **2016**, *11*, 5381; c) S. K. Singh, S. Singh, J. W. Lillard, Jr., R. Singh, *Int J Nanomedicine* **2017**, *12*, 6205.

[3] a) H. Wang, Q. Jia, W. Liu, F. Nan, X. Zheng, Y. Ding, H. Ren, J. Wu, J. Ge, *ChemMedChem* **2020**, *15*, 177; b) C. A. Choi, J. E. Lee, Z. A. I. Mazrad, Y. K. Kim, I. In, J. H. Jeong, S. Y. Park, *ChemMedChem* **2018**, *13*, 1459.

[4] a) X. Xu, R. Ray, Y. Gu, H. J. Ploehn, L. Gearheart, K. Raker, W. A. Scrivens, *J Am Chem Soc* **2004**, *126*, 12736; b) Y. P. Sun, B. Zhou, Y. Lin, W. Wang, K. A. Fernando, P. Pathak, M. J. Meziani, B. A. Harruff, X. Wang, H. Wang, P. G. Luo, H. Yang, M. E. Kose, B. Chen, L. M. Veca, S. Y. Xie, *J Am Chem Soc* **2006**, *128*, 7756.

[5] a) A. D. Veloso, A. M. Ferraria, A. M. Botelho do Rego, P. B. Tavares, P. Valentao, D. D. Pereira, P. B. Andrade, A. J. Fernandes, M. C. Oliveira, R. A. Videira, *ChemMedChem* **2019**, *14*, 699; b) F. Radnia, N. Mohajeri, N. Zarghami, *Talanta* **2020**, *209*, 120547; c) P. Gao, S. Liu, Y. Su, M. Zheng, Z. Xie, *Bioconjug Chem* **2020**, 31, 646.

[6] H. Yao, J. Li, Y. Song, H. Zhao, Z. Wei, X. Li, Y. Jin, B. Yang, J. Jiang, *Int J Nanomedicine* **2018**, *13*, 6249.

[7] M. Farshbaf, S. Davaran, F. Rahimi, N. Annabi, R. Salehi, A. Akbarzadeh, *Artif Cells Nanomed Biotechnol* **2018**, *46*, 1331.

[8] N. Arsalani, P. Nezhad-Mokhtari, E. Jabbari, *Artif Cells Nanomed Biotechnol* **2019**, *47*, 540.

[9] D. Li, P. Jing, L. Sun, Y. An, X. Shan, X. Lu, D. Zhou, D. Han, D. Shen, Y. Zhai, S. Qu, R. Zboril, A. L. Rogach, *Adv Mater* **2018,** *30*, e1705913.

[10] N. L. Teradal, R. Jelinek, *Adv Healthc Mater* **2017**, *6,* 201700574.
[11] a) S. T. Yang, L. Cao, P. G. Luo, F. Lu, X. Wang, H. Wang, M. J. Meziani, Y. Liu, G. Qi, Y. P. Sun, *J Am Chem Soc* **2009**, *131*, 11308; b) Z. A. Qiao, Y. Wang, Y. Gao, H. Li, T. Dai, Y. Liu, Q. Huo, *Chem Commun* **2010**, *46*, 8812.
[12] a) F. Wu, L. Yue, H. Su, K. Wang, L. Yang, X. Zhu, *Nanoscale Res Lett* **2018**, *13*, 357; b) Y. Zhou, P. Y. Liyanage, D. Devadoss, L. R. Rios Guevara, L. Cheng, R. M. Graham, H. S. Chand, A. O. Al-Youbi, A. S. Bashammakh, M. S. El-Shahawi, R. M. Leblanc, *Nanoscale* **2019**, *11*, 22387; c) P. W. Gong, L. Sun, F. Wang, X. C. Liu, Z. Q. Yan, M. Z. Wang, L. Zhang, Z. Z. Tian, Z. Liu, J. M. You, *Chem Eng J* **2019**, *356*, 994.
[13] a) T. Kong, L. Hao, Y. Wei, X. Cai, B. Zhu, *Cell proliferation* **2018**, e12488; b) Y. Yuan, B. Guo, L. Hao, N. Liu, Y. Lin, W. Guo, X. Li, B. Gu, *Colloids Surf B Biointerfaces* **2017**, *159*, 349; c) Q. H. Zeng, D. Shao, X. He, Z. Y. Ren, W. Y. Ji, C. X. Shan, S. N. Qu, J. Li, L. Chen, Q. Li, *J Mater Chem B* **2016**, *4*, 5119.
[14] a) J. Ge, M. Lan, B. Zhou, W. Liu, L. Guo, H. Wang, Q. Jia, G. Niu, X. Huang, H. Zhou, X. Meng, P. Wang, C. S. Lee, W. Zhang, X. Han, *Nat Commun* **2014**, *5*, 4596; b) S. Rondeau-Gagne, J. F. Morin, *Chem Soc Rev* **2014**, *43*, 85; c) S. Zhu, Y. Song, J. Shao, X. Zhao, B. Yang, *Angew Chem Int Ed Engl* **2015**, *54*, 14626.
[15] Y. L. Zhang, X. Zhang, X. Z. Miao, Y. Y. Yuan, J. Gao, X. Li, Y. G. Liu, P. Tan, *J Asian Nat Prod Res* **2019**, 1585820.
[16] P. C. Rao, S. Begum, M. Sahai, D. S. Sriram, *Tumour Biol* **2017**, *39*, 1010428317694565.
[17] a) Q. Cao, S. Hong, Y. Li, H. Chen, Y. Shen, K. Shao, M. Lu, H. Dai, S. Ma, G. Dai, *Rsc Adv* **2018**, *8*, 30937; b) B. Han, P. Jiang, Z. Li, Y. Yu, T. Huang, X. Ye, X. Li, *Phytomedicine* **2018**, *48*, 152.
[18] a) F. N. Chai, W. Y. Ma, J. Zhang, H. S. Xu, Y. F. Li, Q. D. Zhou, X. G. Li, X. L. Ye, *Biomed Pharmacother* **2018**, *103*, 1002; b) L. Zhou, F. Yang, G. Li, J. Huang, Y. Liu, Q. Zhang, Q. Tang, C. Hu, R. Zhang, *Front Pharmacol* **2018**, *9*, 517.
[19] a) Y. T. Zhang, Y. Q. Yu, X. X. Yan, W. J. Wang, X. T. Tian, L. Wang, W. L. Zhu, L. K. Gong, G. Y. Pan, *Acta pharmacol Sin* **2019**, *40*, 133; b) J. Wu, Y. Luo, D. Deng, S. Su, S. Li, L. Xiang, Y. Hu, P. Wang, X. Meng, *J Cell Mol Med* **2019**, 23, 7946.
[20] W. Ren, S. Chen, S. Li, Y. Zhang, J. Liu, M. Guan, H. Yang, N. Li, C. Han, T. Li, Z. Zhao, J. Ge, *Chem Eur J* **2018**, *24*, 15806.
[21] W. Ren, S. Chen, Y. Liao, S. Li, J. Ge, F. Tao, Q. Huo, Y. Zhang, Z. Zhao, *Colloids Surf B Biointerfaces* **2018**, *174*, 384.
[22] J. Ge, Q. Jia, W. Liu, L. Guo, Q. Liu, M. Lan, H. Zhang, X. Meng, P. Wang, *Adv Mater* **2015**, *27*, 4169.
[23] H. Maeda, J. Wu, T. Sawa, Y. Matsumura, K. Hori, *J Control Release* **2000**, *65*, 271.
[24] K. Zou, Z. Li, Y. Zhang, H. Y. Zhang, B. Li, W. L. Zhu, J. Y. Shi, Q. Jia, Y. M. Li, *Acta Pharmacol Sin* **2017**, *38*, 157.
[25] T. Huang, Y. Xiao, L. Yi, L. Li, M. Wang, C. Tian, H. Ma, K. He, Y. Wang, B. Han, X. Ye, X. Li, *Sci Rep* **2017**, *7*, 38524.
[26] a) J. Fang, Y. Liu, Y. Chen, D. Ouyang, G. Yang, T. Yu, *Int J Nanomedicine* **2018**, *13*, 5991; b) X. D. Li, Z. Wang, X. R. Wang, D. Shao, X. Zhang, L. Li, M. F. Ge, Z. M. Chang, W. F. Dong, *Int J Nanomedicine* **2019**, *14*, 3967.
[27] T. Kong, R. Zhou, Y. Zhang, L. Hao, X. Cai, B. Zhu, *Cell prolif* **2019**, e12713.
[28] a) Y. Xu, Y. Shan, H. Cong, Y. Shen, B. Yu, *Curr Pharm Des* **2018**, *24*, 4060; b) J. R. Aguilar Cosme, H. E. Bryant, F. Claeyssens, *PLoS One* **2019**, *14*, e0220210.
[29] Y. Wei, X. Jin, T. Kong, W. Zhang, B. Zhu, *Cell prolif* **2019**, *52*, e12586.
[30] X. Yuan, Q. Xie, K. Su, Z. Li, D. Dong, B. Wu, *Int J Nanomedicine* **2017**, *12*, 4981.

Entry for the Table of Contents

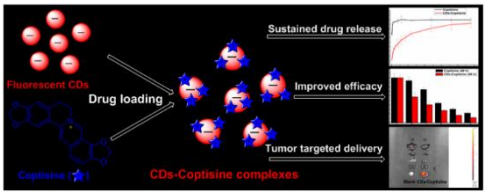

Schematic illustration of polymers based red emissive CDs loading coptisine for efficient cancer therapy.